

The oxygen-18 isotope approach for measuring aquatic metabolism in high-productivity waters

Craig R. Tobias,¹ John Karl Böhlke, and Judson W. Harvey
U.S. Geological Survey, 431 National Center, Reston, Virginia 20192

Abstract

We examined the utility of $\delta^{18}\text{O}_2$ measurements in estimating gross primary production (P), community respiration (R), and net metabolism (P:R) through diel cycles in a productive agricultural stream located in the midwestern U.S.A. Large diel swings in O_2 ($\pm 200 \mu\text{mol L}^{-1}$) were accompanied by large diel variation in $\delta^{18}\text{O}_2$ ($\pm 10\text{‰}$). Simultaneous gas transfer measurements and laboratory-derived isotopic fractionation factors for O_2 during respiration (α_r) were used in conjunction with the diel monitoring of O_2 and $\delta^{18}\text{O}_2$ to calculate P, R, and P:R using three independent isotope-based methods. These estimates were compared to each other and against the traditional “open-channel diel O_2 -change” technique that lacked $\delta^{18}\text{O}_2$. A principal advantage of the $\delta^{18}\text{O}_2$ measurements was quantification of diel variation in R, which increased by up to 30% during the day, and the diel pattern in R was variable and not necessarily predictable from assumed temperature effects on R. The P, R, and P:R estimates calculated using the isotope-based approaches showed high sensitivity to the assumed system fractionation factor (α_r). The optimum modeled α_r values (0.986–0.989) were roughly consistent with the laboratory-derived values, but larger (i.e., less fractionation) than α_r values typically reported for enzyme-limited respiration in open water environments. Because of large diel variation in O_2 , P:R could not be estimated by directly applying the typical steady-state solution to the O_2 and ^{18}O - O_2 mass balance equations in the absence of gas transfer data. Instead, our results indicate that a modified steady-state solution (the daily mean value approach) could be used with time-averaged O_2 and $\delta^{18}\text{O}_2$ measurements to calculate P:R independent of gas transfer. This approach was applicable under specifically defined, net heterotrophic conditions. The diel cycle of increasing daytime R and decreasing nighttime R was only partially explained by temperature variation, but could be consistent with the diel production/consumption of labile dissolved organic carbon from photosynthesis.

Gross primary production (P) and community respiration (R) are central regulators of biogeochemical turnover in aquatic environments on local to regional scales (del Giorgio et al. 1997; Duarte and Agusti 1998; Cole et al. 2000). The balance between P and R (i.e., net metabolism) provides an indicator of nutrient enrichment, trophic status, allochthonous organic carbon utilization, and overall water quality (del Giorgio and Peters 1994; Hanson et al. 2003). Accurate estimates of P and R are needed to assess carbon, oxygen, and nutrient processing on watershed scales (Mulholland et al. 1997; Sabater et al. 2000; Hall and Tank 2003).

¹To whom correspondence should be addressed. Present address: Department of Earth Sciences, University of North Carolina–Wilmington, Wilmington, North Carolina 28403 (tobiasc@uncw.edu).

Acknowledgments

Stanley Mroczkowski, Tyler Coplen, Karen Casciotti, Mary Voytek, Julie Kirshtein, Richard L. Smith, Deborah Repert, Jessica Newlin, Joel Detty, and Peggy Widman contributed to this work. We also thank Richard L. Smith, Holly Weyers, and two anonymous reviewers for their insightful comments on previous versions of this manuscript.

This study was supported by the U.S. Department of Agriculture Cooperative State Research, Education, and Extension Service (National Research Initiative Competitive Grants Program in Watershed Processes and Water Resources), and by the U.S. Geological Survey National Research Program in Water Resources, through the National Research Council post-doctoral fellowship program.

In situ estimates of P and R traditionally have relied upon O_2 budgets that balanced sources and sinks of O_2 (e.g., photosynthesis and respiration) with O_2 exchange (invasion or evasion) between water and the atmosphere. For experimental purposes in the current study, as in most previous studies of this type, P is defined as O_2 production (including photosynthesis but excluding other non-oxygenic primary production pathways), and R is defined as O_2 reduction (including O_2 respiration and chemical O_2 demand but excluding other respiration reactions such as denitrification). Many of the previous reach-scale stream metabolism measurements have employed variants of the diel O_2 change technique (Odum 1956; Marzolf et al. 1994; Mulholland et al. 2001). The diel O_2 approach has yielded estimates of metabolism balance (P:R) as well as daily rates of P and R, provided that gas transfer (i.e., the reaeration coefficient k_{O_2}) was known. Because R is difficult to resolve from P when both are active (i.e., during daytime), most experimental approaches include assumptions about how R varies during daytime. Common approaches include: (1) assuming that daytime R equal nighttime R; (2) deriving daytime R from the observed nighttime relationship between R and temperature; and (3) applying a Q_{10} temperature function (e.g., $Q_{10} = 2$) for R throughout the diel cycle. These different assumptions may be problematic if R is tightly coupled to contemporaneous production and release of photosynthetic carbon (del Giorgio and Williams 2005; Pace and Prairie 2005), if photorespiration pathways comprise a large fraction of total O_2 demand (Raven and Beardall 2005), and/or if R responds unpredictably to diel temperature variation. An

approach that estimates diel R variation but is not formally dependent on these assumptions would provide a basis for subsequent investigation of respiration pathways and/or controls on R.

Measuring the isotopic composition of dissolved O₂ ($\delta^{18}\text{O}_2$) may resolve some of the uncertainties of P and R determinations. Photosynthesis (i.e., gross primary production; GPP) adds O₂ to the dissolved O₂ pool that is isotopically identical to the source H₂O. Respiration preferentially removes ¹⁶O, thereby enriching the residual dissolved O₂ pool in ¹⁸O (Kiddon et al. 1993; Parker et al. 2005; and others). These effects are further modified by gas transfer. Strongly net heterotrophic systems ($P \ll R$ and $R \gg$ gas transfer) will thus have high $\delta^{18}\text{O}_2$ values, whereas strongly autotrophic systems ($P \gg R$ and $P \gg$ gas transfer) will have low $\delta^{18}\text{O}_2$ values. The $\delta^{18}\text{O}_2$ in gas transfer-dominated systems will approach that of air equilibrated water (+24.5‰_{vsmow}).

Two options exist for incorporating O₂ isotope measurements into metabolism calculations. The first approach uses “exact solutions” to O₂ and O₂ isotope mass balance equations. It yields estimates of instantaneous P and R, and requires a gas transfer estimate. This approach has not been widely used, but has the potential for better characterizing diel variation in R and improving subsequent metabolism calculations that rely on R. A second approach that has been used previously relies on a steady-state solution to the O₂ and O₂ isotope mass balance equations. It yields an estimate of the net daily P:R ratio ($P:R_{24}$) without independent knowledge of gas transfer, and is appropriate when O₂ concentrations are near steady state (Quay et al. 1995; Russ et al. 2004). This technique can potentially remove uncertainties associated with gas transfer and has utility in systems where k_{O_2} is difficult to measure directly, but it does not yield independent P and R rates. A further potential complication of this approach is that O₂ tends to deviate from steady state in high productivity waters.

Both of these O₂ isotope applications require estimation of the O isotopic fractionation during respiration (α_r). The calculated P, R, and P:R ratio may be variably sensitive to estimates of α_r depending upon the importance of R relative to P and gas transfer. Although several estimates of α_r have been used in metabolism calculations across a range of large aquatic systems (e.g., Quay et al. 1995; Wang and Veizer 2000; Russ et al. 2004), these values represent water column processes and typically are similar to enzyme-limited fractionations with α_r near 0.98. Those α_r values may not be appropriate for shallow systems where benthic processes are important. Respiration in such environments may be limited by O₂ flux into sediments (a non-isotope fractionating process), be composed of variable contributions from photorespiration and heterotrophic respiration sources with different α_r values (Raven and Beardall 2005), or be subject to chemical oxygen demand in the streambed. It is not clear how useful, and in what form, the addition of $\delta^{18}\text{O}_2$ and α_r data will be for evaluating metabolism in such systems.

In an effort to examine diel variability in R, and to improve reach-scale metabolism estimates in these types of

environments, we combined diel O₂ and gas transfer measurements with diel isotopic analyses of $\delta^{18}\text{O}_2$. Experiments were done at multiple locations and times in a productive, second-order agricultural stream located in mid-continent North America. We applied several different types of mathematical models to determine the various metabolism parameters with and without isotopes.

Methods

To estimate time variable rates of P, R, and P:R, we measured in-stream gas transfer, conducted diel monitoring of stream O₂ concentration and $\delta^{18}\text{O}_2$, and experimentally determined the isotopic fractionation factor for O₂ respiration. All field measurements occurred within a 1-km reach of Sugar Creek in western Indiana, U.S.A. (40°40'31"N, 87°18'27"W) in June and September 2003. Watershed land use is >90% row-crop agriculture. Sugar Creek is a low-gradient, channelized stream with a streambed composed of coarse sand and fine gravel. All sampling was conducted during baseflow conditions ($Q \sim 15\text{--}50 \text{ L s}^{-1}$) with a mean stream depth of 15–20 cm. Sampling stations divided the 1-km stream reach into two and three subreaches in June and September, respectively (Fig. 1). The study reach between sites B and C (Fig. 1) supported extensive autotrophic communities including benthic microalgae (pennate diatoms), chlorophyte macroalgae, and vascular macrophyte beds of *Elodea* spp. Autotrophic communities were less abundant between sites A and B (Fig. 1).

Dissolved O₂ analysis—For periods of 24–120 h, dissolved O₂ and water temperature were recorded at 10-min intervals at several stations (sites B and C in June, and sites A and C in September) with a Hydrolab DS4 and YSI 600XL data sondes. Dissolved gas measurements were performed using gas chromatography (GC) on additional samples collected at 1–3-h intervals in 160-mL serum bottles preserved with KOH (<http://water.usgs.gov/lab/dissolved-gas>). These GC-determined O₂ concentrations were used to adjust for drift in the O₂ sondes during the study.

Isotope analysis— $\delta^{18}\text{O}$ values for dissolved O₂ (designated as $\delta^{18}\text{O}_2$) were determined on serum bottle headspace after GC analysis using a Finnigan Delta XP isotope ratio mass spectrometer (IRMS) fitted with a Tekmar 7000 headspace sampler and Finnigan GC–GP interface. A closed loop in the headspace sampler was used to pressurize the headspace and inject aliquots into a 5-Å mole-sieve capillary gas chromatograph that separated N₂ from (O₂ + Ar) (modified from Revesz et al. 1999). The IRMS was operated in continuous-flow mode and configured to monitor ion beams simultaneously at m/z (mass/charge) 28, 29, 32, 34, 36, and 40. Air-equilibrated water standards were interspersed with the stream samples.

Representative streamwater samples were also collected in June and September for $\delta^{18}\text{O}$ analysis of the H₂O. Isotope analyses of water were done by the CO₂ equilibration technique (Epstein and Mayeda, 1953) using

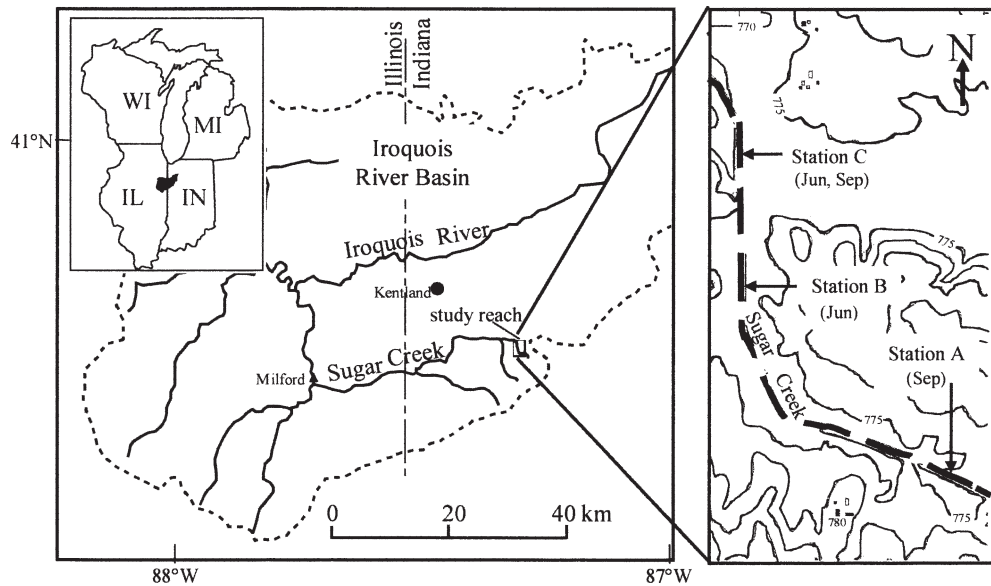


Fig. 1. Site map.

a Dupont 21-491 IRMS in dual inlet mode (<http://isotopes.usgs.gov>). All $\delta^{18}\text{O}$ values (O_2 and H_2O) are reported in delta notation relative to Vienna Standard Mean Ocean Water (VSMOW).

$$\delta^{18}\text{O} = \left(\frac{R_{\text{sample}}}{R_{\text{std}}} - 1 \right) \quad (1)$$

where R_{sample} is the $^{18}\text{O}:^{16}\text{O}$ ratio of dissolved O_2 or H_2O in the sample, and R_{std} is $^{18}\text{O}:^{16}\text{O}$ of VSMOW (0.002005). $\delta^{18}\text{O}_2$ and $\delta^{18}\text{O}\text{-H}_2\text{O}$ are reported in parts per thousand (‰) with precision of approximately 0.3‰ and 0.1‰, respectively.

Isotope fractionation experiments—The apparent isotope fractionation factor (α_r) for O_2 respiration was determined in several incubation experiments using Sugar Creek sediments. The approach consisted of incubating sediments and air-equilibrated water in a closed system in the dark and calculating α_r from changes in O_2 and $\delta^{18}\text{O}_2$ as related by the Rayleigh equation.

$$\ln \left[\frac{\delta^{18}\text{O}_{2,t} + 1}{\delta^{18}\text{O}_{2,t_0} + 1} \right] = \varepsilon \ln f \quad (2)$$

where $\delta^{18}\text{O}_{2,t_0}$ and $\delta^{18}\text{O}_{2,t}$ are the isotope values for dissolved O_2 at the start and end of an incubation period t , and f is the fraction of original O_2 remaining. The enrichment factor (ε) for O_2 respiration (in ‰) is related to the fractionation factor α by $\alpha = 1 + \varepsilon$. Because the apparent fractionation factor in the stream may be affected by various physical and chemical conditions during respiration (e.g., diffusive transport, mineral oxidation, etc.), several incubation conditions and sediment:water ratios were used to provide estimates of α_r , including static core and sediment slurries. For the core incubations, intact cores (30-cm depth, $n = 8$) were incubated with overlying stream water and zero headspace. The overlying water was

sampled for O_2 and $\delta^{18}\text{O}_2$ at 2-h intervals until approximately 80% of the dissolved O_2 had been consumed. O_2 and $\delta^{18}\text{O}_2$ values were determined using GC and GC-IRMS as described above. Sediment slurry incubations were performed with the upper 2 cm of streambed sediments. Approximately 5–7 g (wet weight) of homogenized sediment was incubated with 150 mL of deionized water or 0.2- μm -filtered stream water in serum bottles with zero headspace. Slurry incubations were done at 22°C and kept in varying states of suspension using a shaker table or rotating incubator. At approximately 30-min intervals, triplicate bottles were sacrificed by unsealing and pumping 15 mL water into He-flushed, sealed, 30-mL serum bottles containing KOH. Headspace was extracted for IRMS analysis of O_2/Ar and $\delta^{18}\text{O}_2$. In total, four incubation experiments were done to estimate α_r .

Data analysis

Four different approaches were used to synthesize the data and derive estimates of P, R, and P:R ratios.

Approach no. 1: diel mass balance of O_2 —This approach, which does not include $\delta^{18}\text{O}_2$, has been used in numerous stream studies and is described in detail elsewhere (McCutchan et al. 2002; Hall and Tank 2005; McCutchan and Lewis 2006). This approach for estimating P, R, and P:R requires diel O_2 records and an estimate of O_2 gas transfer and can be approximated by (McCutchan et al. 2003; Hall and Tank 2005)

$$\frac{d\text{O}_2}{dt} = k_{\text{O}_2}(\text{O}_{2,s} - \text{O}_2) - R + P + G(\text{O}_{2,gw} - \text{O}_2) \quad (3)$$

where $\frac{d\text{O}_2}{dt}$ is the change in dissolved O_2 concentration over time ($\mu\text{mol O}_2 \text{ L}^{-1}$), k_{O_2} is the O_2 gas transfer

coefficient (i.e., reaeration coefficient; time^{-1}), $O_{2, \text{gw}}$ is the assumed O_2 concentration of groundwater discharge, whereas O_2 and $O_{2, \text{s}}$ are the O_2 concentrations measured in the stream and calculated for air-saturated water at the current time, respectively. G is the fractional increase in stream flow due to groundwater discharge (time^{-1}). Values of $O_{2, \text{s}}$ were calculated at 10-min intervals from measured stream temperatures and the average daily atmospheric pressure using solubility data from Weiss (1970). Groundwater contributions (G) and the aeration coefficient (k_{O_2}) were estimated from Br and SF₆ tracer additions conducted during the diel O_2 and $\delta^{18}O_2$ monitoring. Daytime R in the O_2 mass balance was treated in three separate ways: (1) R was held constant throughout the diel cycle; (2) R was permitted to vary according to a linear relation established between R and observed temperature at night; and (3) R was permitted to vary according to the Q_{10} equation

$$R = R_{20} \times Q_{10}^{[(T - 20)/10]} \quad (4)$$

where R_{20} is respiration at night at the near-average stream temperature of 20°C, and Q_{10} is the constant defining the temperature effect on R and was set at a value of 2.0.

Because O_2 changes occurred rapidly with changing temperature and light, but more gradually with distance downstream, we used the single-point version of the O_2 mass balance approach at each station (Hornberger and Kelly 1975; Young and Huryn 1999; Mullholland et al. 2005), in which dO_2/dt was defined as the difference between successive measurements at a given location.

Approach no. 2: exact (inverse) solution incorporating $\delta^{18}O_2$ —The diel $\delta^{18}O_2$ monitoring permitted the addition of the following isotope mass balance equation:

$$\frac{d^{18}[O_2]}{dt} = k_{O_2} \alpha_g (O_{2, \text{s}}^{18:16} O_a \alpha_s - O_2^{18:16} O) - R^{18:16} O \alpha_r \quad (5)$$

$$+ P^{18:16} O_w \alpha_p + G(O_{2, \text{gw}}^{18:16} O_{\text{gw}} - O_2^{18:16} O)$$

where $\frac{d^{18}[O_2]}{dt}$ is the change in the ^{18}O content of dissolved stream O_2 between sampling times, and $^{18:16}O$, $^{18:16}O_a$, $^{18:16}O_{\text{gw}}$, and $^{18:16}O_w$ are the isotope ratios (approximately equal to the ^{18}O mole fractions) in stream O_2 , atmospheric O_2 , groundwater O_2 , and H_2O , respectively. The isotope fractionation factors for O during gas transfer ($\alpha_g = 0.9972$), dissolution ($\alpha_s = 1.0007$), and photosynthesis ($\alpha_p = 1.000$) are summarized in Benson and Krause (1984); Knox et al. (1992); Guy et al. (1993); and Quay et al. (1995). Values of α_r were assumed to be constant through the diel cycle and were derived either from the incubation experiments or, alternatively, by least squares minimization of nighttime P in the exact inverse solution. Combining Eq. 3 and 5 provided exact solutions for P and R for each time step according to Eq. 6 and 7.

$$P = \frac{dO_2}{dt} - k_{O_2}(O_{2, \text{s}} - O_2) + R - G(O_{2, \text{gw}} - O_2) \quad (6)$$

$$R = \frac{\frac{d^{18}[O_2]}{dt} - k_{O_2} \alpha_g (O_{2, \text{s}}^{18:16} O_a \alpha_s - O_2^{18:16} O)}{^{18:16}O_w \alpha_p - ^{18:16}O \alpha_r} - \frac{G(O_{2, \text{gw}}^{18:16} O_{\text{gw}} - O_2^{18:16} O) - \frac{dO_2}{dt} ^{18:16} O_w \alpha_p}{^{18:16}O_w \alpha_p - ^{18:16}O \alpha_r} \quad (7)$$

$$+ \frac{k_{O_2}(O_{2, \text{s}} - O_2)^{18:16} O_w \alpha_p}{^{18:16}O_w \alpha_p - ^{18:16}O \alpha_r}$$

$$+ \frac{^{18:16}O_w \alpha_p G(O_{2, \text{gw}} - O_2)}{^{18:16}O_w \alpha_p - ^{18:16}O \alpha_r}$$

As with all the approaches, $\frac{dO_2}{dt}$ and/or $\frac{d^{18}[O_2]}{dt}$ were treated as finite differences. The 1–3 h $\delta^{18}O_2$ data were interpolated to 10-min values through a tight functional relationship to O_2 concentration at each site for each diel cycle.

Approach no. 3: time-forward numerical simulation— P , R , and $P:R$ were determined by constructing a numerical spreadsheet reaction model to simulate changes in O_2 concentration and $\delta^{18}O_2$ over the diel cycle and minimizing differences between simulated and measured values. This model is similar to the one described by Böhlke et al. (2004) in which O_2 production, consumption, gas transfer, and groundwater discharge parameters are expressed as vertical fluxes entering or leaving the water column, and used to calculate changes in the concentrations of each of the isotopic species in the stream through a series of time steps. Changes in concentration of dissolved O_2 are given by

$$C_t = Q_{t-\Delta t}/Q_t \times (C_{t-\Delta t} + C_{GRP} + \Delta C_a) \quad (8)$$

$$\Delta C_{GRP} = \Delta t/Z \times (F_G + F_R + F_P) \times 10^{-3} \quad (9)$$

$$\Delta C_a = \Delta t/Z \times GTV_t \times (C_{eq,t} - (C_{t-\Delta t} + \Delta C_{GRP})) \quad (10)$$

where C is concentration in $\mu\text{mol L}^{-1}$; t is time in h; Δt is one time step (0.05–0.10 h); Z is mean stream depth in m; GTV is the gas transfer velocity in m h^{-1} ; F is vertical flux in $\mu\text{mol m}^{-2} \text{h}^{-1}$; and the subscripts G , R , P , and A refer to groundwater discharge, O_2 reduction (R), O_2 production (P), and air–water exchange, respectively. These equations were solved independently for total O , ^{18}O , and ^{16}O by using the isotope fractionation factors (α) to define the equilibrium states and to adjust the gas transfer and reaction rates (k).

$$\alpha = k(^{18}O)/k(^{16}O) \quad (11)$$

In various simulations, F_R was either held constant or defined as a function of stream temperature using Eq. 4. F_P was defined as a hyperbolic tangent function of irradiance (Jassby and Platt 1976)

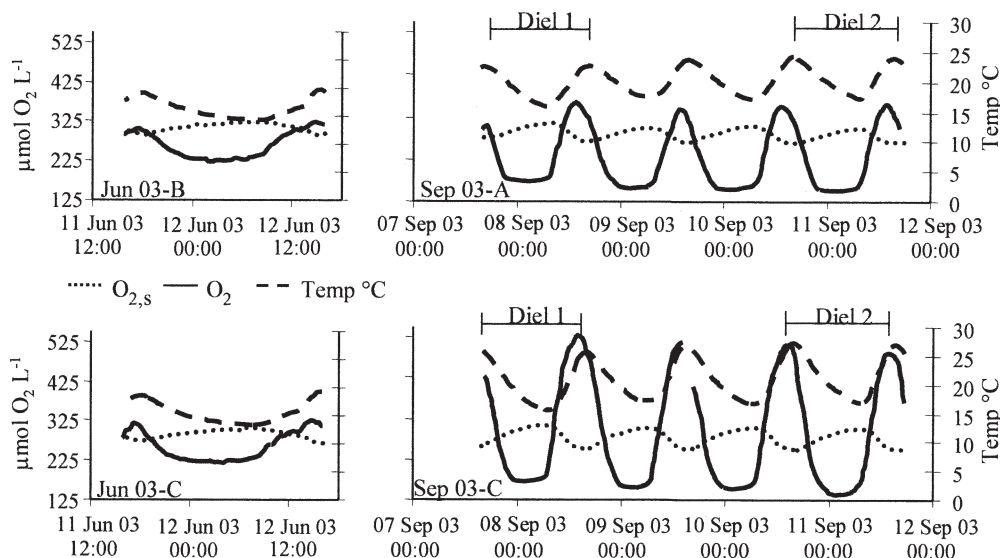


Fig. 2. Diel oxygen and temperature data for all sampling sites in June and September 2003. $O_{2,s}$ is the air-saturated O_2 concentration calculated from temperature, barometric pressure, and relative humidity (Weiss 1970). Two diel periods were examined in September; they are designated as Diel 1 (D1) and Diel 2 (D2).

$$P = P_m \tanh \left[a \left(\frac{I}{P_m} \right) \right] \quad (12)$$

using irradiance data (<http://agmetx.agry.purdue.edu/sc.index.html>) from West Lafayette (~40 km southwest of the site). Model optimization (e.g., P, R, Q_{10}) was achieved by using a least squares routine (Microsoft Excel Solver) to minimize the cumulative absolute differences between the observed and simulated O_2 and $\delta^{18}O_2$ values through a complete diel cycle.

Approach no. 4: steady-state approximation of P:R—Assuming steady-state O_2 ($dO_2/dt = 0$), the P:R ratio can be determined from the O_2 and $\delta^{18}O_2$ in the absence of k_{O_2} (Quay et al. 1995):

$$P : R_{ss} = \frac{{}^{18:16}O\alpha_r - {}^{18:16}O_g}{{}^{18:16}O_w - {}^{18:16}O_g} \quad (13)$$

where ${}^{18:16}O_g$ is the ratio of the net air-water fluxes of ${}^{18,16}O_2$ and ${}^{16,16}O_2$ defined as

$${}^{18:16}O_g = \frac{\alpha_r \left[{}^{18:16}O_a \alpha_s - \left(\frac{O_2}{O_{2,s}} \right) {}^{18:16}O \right]}{\left[1 - \left(\frac{O_2}{O_{2,s}} \right) \right]} \quad (14)$$

The steady-state solution was applied in two ways. First, Eq. 13 and 14 were used to calculate P:R_{ss} at each time interval for comparison to instantaneous P:R ratios determined by the other models. This application tested the uncertainty in P:R_{ss} generated by the steady-state model in systems that deviated to varying degrees from steady-state conditions. Second, time weighted daily mean values (dmv) of O_2 concentration and $\delta^{18}O_2$ were used as inputs for Eq. 13 and 14 to calculate 24-h integrated P:R₂₄,

^{ss-dmv}. This dmv variant of the steady-state solution was assessed because of the potential for encountering non-steady state environments where diel O_2 and $\delta^{18}O_2$ can be measured, but gas transfer cannot be readily determined (e.g., large shallow rivers or estuaries).

Results

Inputs for determining metabolism parameters

Physical characteristics—Sugar Creek in June was colder, faster, and deeper than in September (Fig. 2; Table 1). The reaeration coefficient (k_{O_2}) and gas transfer velocity (GTV) were higher in June by a factor of 2 and 3, respectively (Table 1).

Oxygen concentration—Diel O_2 varied considerably between June and September and between upstream and downstream reaches (Fig. 2). The downstream site (C) always showed a larger diel O_2 swing than the upstream sites (A and B). Greater productivity in the downstream reach likely reflected higher autotrophic biomass between sites B and C. Lower irradiance and higher gas transfer in June relative to September contributed to the smaller difference between minimum and maximum O_2 concentrations. June measurements were dominated by O_2 below

Table 1. Mean gas transfer (GTV) and stream characteristics for Sugar Creek.

	GTV (m h ⁻¹)	Mean depth (m)	k_{O_2} (h ⁻¹)	Velocity (m s ⁻¹)
June 2003	0.162	0.20	0.81	0.14
September 2003	0.057	0.15	0.39	0.06

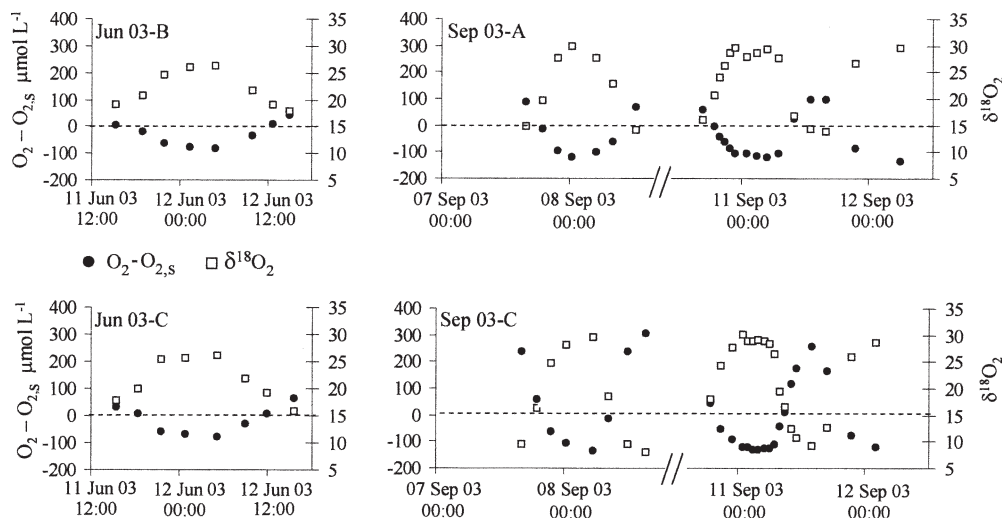


Fig. 3. Diel $\delta^{18}\text{O}_2$ (in ‰ VSMOW) and oxygen subsidy (or deficit), relative to air saturation, for all sampling sites in June and September 2003.

saturation with nighttime minima near $225 \mu\text{mol O}_2 \text{ L}^{-1}$ ($\sim 100 \mu\text{mol O}_2 \text{ L}^{-1}$ below O_{2s}). Higher daytime highs and lower nighttime lows for O_2 were measured in September. Nighttime O_2 fell to a constant low near $175 \mu\text{mol O}_2 \text{ L}^{-1}$ ($\sim 150 \mu\text{mol O}_2 \text{ L}^{-1}$ below O_{2s}). O_2 peaked around 14:30 h each day at approximately $400 \mu\text{mol O}_2 \text{ L}^{-1}$ and $525 \mu\text{mol O}_2 \text{ L}^{-1}$ for sites A and C, respectively. The stream was oversaturated in O_2 by nearly two-fold at peak O_2 . The highest measured O_2 concentrations may yield minimum estimates of O_2 production because of bubble formation and loss, but this effect could not be quantified in this study.

Isotopes—Diel $\delta^{18}\text{O}_2$ varied inversely with O_2 concentration and the magnitude of O_2 oversaturation (Figs. 3, 4). The minimum values for $\delta^{18}\text{O}_2$ were measured in the late afternoon, and the maximum values for $\delta^{18}\text{O}_2$ occurred in the early morning just before sunrise. These daily $\delta^{18}\text{O}_2$ excursions ranged from a low of 9‰ to a high of 30‰, with the largest swings coincident with the largest O_2 changes. The $\delta^{18}\text{O}_2$ values were significantly correlated to O_2 concentrations ($p < 0.0001$) at each site for any given 24-h period. The functional dependence of $\delta^{18}\text{O}_2$ on O_2 concentration could be represented with 2nd or 3rd order regression equations ($r^2 = 0.999$) depending on the site and diel cycle. These regression equations were used in the exact inverse solution and the time-forward model simulations to interpolate the record of $\delta^{18}\text{O}_2$ between the 1–3 hourly sampling times. Three processes influenced the relationship between $\delta^{18}\text{O}_2$ and O_2 concentration (Fig. 4). Isotope fractionation during respiration increased $\delta^{18}\text{O}_2$ through the night. The $\delta^{18}\text{O}_2$ decreased during the day when photosynthesis added O_2 with low $\delta^{18}\text{O}$ from stream H_2O to the dissolved O_2 pool. Streamwater collected at various times during all of the monitoring periods had a constant combined average $\delta^{18}\text{O}-\text{H}_2\text{O}$ of -6.9‰ (± 0.1 , $n = 16$). Gas transfer pulled the O_2 and $\delta^{18}\text{O}_2$ towards air saturated values at all times. Therefore, although $\delta^{18}\text{O}_2$ and O_2 were

well correlated, no single process (isotope fractionation, mixing of sources, or partial equilibration) could be used to describe the array of data.

The fractionation factor (α_r)—Four different α_r values were calculated from the four laboratory incubation experiments and ranged from 0.982 to 0.996 (Table 2).

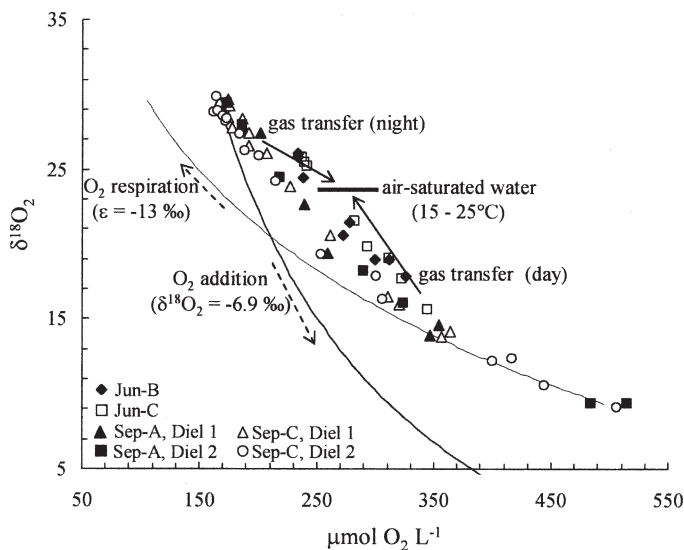


Fig. 4. $\delta^{18}\text{O}_2$ (in ‰ VSMOW) versus O_2 concentration. Air saturated values (solid horizontal line) were calculated for the temperature range in Sugar Creek across study periods. Curves and arrows indicate representative isolated trajectories corresponding to photosynthesis (addition of O_2 with $\delta^{18}\text{O}_2 = -6.9\text{‰}$); O_2 respiration with isotopic fractionation factor $\epsilon = -13\text{‰}$ ($\alpha = 0.987$); and air–water exchange of O_2 (gas transfer). All of these processes operate simultaneously throughout the diel cycle to generate the observed $\delta^{18}\text{O}_2$ values and O_2 concentrations in the stream. The gas transfer arrows show the trajectory caused by increasing reaeration starting with either daytime or nighttime values.

Table 2. O₂ respiration fractionation summary.

	Incubation treatment	Enrichment factor ‰ (ε)	Fractionation factor (α)
June 2003	Core	-11.9	0.988
September 2003	Slurry (field)	-9.4	0.991
September 2003	Core	-14.3	0.986
September 2003	Slurry (lab)	-18.3	0.982
Mean	All treatments	-13.5±2.1	0.987±0.002

The measured α_r values did not group by study period (June vs. September), or by experimental condition (core vs. slurry). The measured α_r values were substantially larger (less fractionation of residual O₂) than previously reported water-column and enzyme-limited effects ($\alpha_r = 0.977$ – 0.980). As described below, the model α_r values did not match exactly any of the individual experimental determinations, but they were similar to the mean of the experimental results ($\alpha_r = 0.987$).

Metabolism model results

Estimates of the various metabolic parameters (Tables 3, 4) were compared among the O₂ mass balance, exact inverse solution, steady-state approximation, and time-forward simulation model approaches. An important consideration in all of the models is the composition of groundwater inputs. Although most upwelling groundwater beneath the stream was anoxic (Böhlke et al. 2004; this study), there were numerous seeps and other shallow discharges that may have contributed oxygenated water to the stream. Because the proportion of each of these groundwater sources is difficult to quantify at the reach scale, we considered three possible groundwater cases (oxic, anoxic, and no groundwater) in the cross-method comparison between isotope approaches. Consistent with the model results of McCutchan et al. (2002) and Hall and Tank (2005), the groundwater inputs to Sugar Creek shifted P:R₂₄ values approximately 15% when O_{2,gw} was assumed to be hypoxic or anoxic, but not substantially when O_{2,gw} was assumed to be air-saturated (Table 4). The R₂₄ values were affected, whereas P₂₄ was affected minimally by changes in O_{2,gw}.

The O₂ mass balance approach estimated metabolism parameters using the diel O₂ data (no isotopes), k_{O₂}, and the various diel R assumptions (Table 4). Highest values of R were measured in June in the upstream reach. The P₂₄

values were highest in September, and always greatest at the downstream (site C) regardless of month. The P:R₂₄ ratios indicated the strongest net heterotrophy in June (P:R = 0.47–0.63), moderate net heterotrophy for site A in September (0.73–0.77), and net autotrophy at site C in September (1.09–1.35). Differences in P:R₂₄ ratios among sites and times in September reflect differences primarily in P, whereas P:R₂₄ ratios were affected by both P and R differences between June and September. The different assumptions for diel R yielded R₂₄ and P₂₄ estimates that varied from <2% (e.g., September A, D1) to almost 30% (June C). P₂₄ differences mimicked R₂₄ differences among the different diel R treatments. Therefore, the different R assumptions affected the P:R₂₄ ratios less than the individual R₂₄ or P₂₄ values, yielding P:R₂₄ ratios that varied typically less than 7% and no more than 15%.

The exact inverse solution approach estimated metabolism parameters using the diel O₂ data, δ¹⁸O₂, α_r, and k_{O₂}. Diel variations in P and R were calculated directly from measurements at 10-min intervals rather than by adopting any assumed functional relations. The P and R rates were highly sensitive to the choice of α_r (Fig. 5). Solution-optimized α_r values for September A and C were between 0.986 and 0.988. Optimum June α_r values were 0.989 and 0.993 for sites B and C, respectively. Uncertainty in the α_r (i.e., assigning the wrong α_r; Fig. 5 c–f) changed the magnitude of all metabolism parameters. Applying a predominantly diffusion-limited end-member α_r of 0.997 (Brandes and Devol 1997) to the September data caused P at night to become negative and flattened R to a constant value from day to night (Fig. 5 c,d). The P:R₂₄ decreased as did the total P₂₄ and R₂₄ (by almost half). Applying a predominantly enzyme-limited end-member α_r of 0.977 (Fig. 5 e,f; Kiddon et al. 1993; Luz et al. 2002; Russ et al.

Table 3. Definition of metabolism parameters. Rates are shown normalized to volume and/or to area to facilitate comparison with existing literature. Stream depths for June or September are used to convert between volumetric and areal rates.

Parameter	Term*	Units
Gross primary production (instantaneous)	P	μmol O ₂ L ⁻¹ , μmol O ₂ m ⁻² h ⁻¹
Community respiration (instantaneous)	R	μmol O ₂ L ⁻¹ , μmol O ₂ m ⁻² h ⁻¹
Daily integrated P	P ₂₄	mmol O ₂ m ⁻² d ⁻¹
Daily integrated R	R ₂₄	mmol O ₂ m ⁻² d ⁻¹
Trophic status (P:R)	P:R	unitless
Daily integrated P:R	P:R ₂₄	unitless

* All terms may carry an additional subscript to denote the method used for their calculation (e.g., “exact” is exact inverse solution; “ss-dmv” is the steady-state solution using daily mean values).

Table 4. Metabolism summary (mmol O₂ m⁻² h⁻¹).

		O ₂ mass balance	Exact isotope solution	Time-forward model	Steady-state (dmv) isotope solution
Jun B	P ₂₄	5.17,*† 6.01,*‡ 3.84*§	6.56*		
Jun B	R ₂₄	10.91,*† 11.51,*‡ 9.31*§	11.85*		
Jun B	P:R ₂₄	0.47,*† 0.52,*‡ 0.41*§	0.56*		0.57*
Jun C	P ₂₄	5.72,*† 6.51,*‡ 4.33*§	5.89*		
Jun C	R ₂₄	9.46,*† 10.41,*‡ 7.69*§	9.10*		
Jun C	P:R ₂₄	0.60,*† 0.63,*‡ 0.56*§	0.64*		0.65*
Sep A–Diel 1	P ₂₄	4.24,*† 4.94,*‡ 4.79*§	6.3*		
Sep A–Diel 1	R ₂₄	5.49,*† 6.41,*‡ 6.48*§	7.81*		
Sep A–Diel 1	P:R ₂₄	0.77,*† 0.77,*‡ 0.74*§	0.81*		0.65*
Sep A–Diel 2	P ₂₄	4.64,*† 5.37,*‡ 5.04*§	5.11, 5.09,¶ 5.37*	5.60, 5.60,¶ 5.25*	
Sep A–Diel 2	R ₂₄	6.25,*† 7.18,*‡ 6.93*§	6.88, 7.55,¶ 7.7*	6.15, 7.70,¶ 7.23*	
Sep A–Diel 2	P:R ₂₄	0.74,*† 0.75,*‡ 0.73*§	0.74, 0.67,¶ 0.69*	0.91, 0.73,¶ 0.73*	0.66*
Sep C–Diel 1	P ₂₄	8.34,*† 9.68,*‡ 9.34*§	11.66*		
Sep C–Diel 1	R ₂₄	6.39,*† 7.93,*‡ 6.93*§	9.2*		
Sep C–Diel 1	P:R ₂₄	1.31,*† 1.22,*‡ 1.35*§	1.27*		1.57*
Sep C–Diel 2	P ₂₄	7.99,*† 8.82,*‡ 8.59*§	8.85, 8.99,¶ 9.02*	9.33, 9.36,¶ 8.88*	
Sep C–Diel 2	R ₂₄	7.32,*† 8.01,*‡ 7.53*§	6.78, 7.61,¶ 8.08*	7.17, 8.76,¶ 8.29*	
Sep C–Diel 2	P:R ₂₄	1.09,*† 1.10,*‡ 1.14*§	1.31, 1.18,¶ 1.12*	1.30, 1.07,¶ 1.07*	1.28*

* Daytime R = Night R.

† Daytime R calculated from Q₁₀ = 2.

‡ Daytime R = Extrapolated from linear night R versus temperature.

§ Groundwater inputs assumed to be §anoxic, ||oxic (equal to stream O₂), ¶no groundwater.

2004) yielded high P values at night (not reasonable) and added severe instability (both positive and negative) to calculated daytime P and R. Only at or very near the optimized α_r of 0.986–0.988 (September) could reasonable P₂₄, R₂₄, and P:R₂₄ values be achieved (Table 4) with a nighttime P at or near zero. At the optimum α_r for each site, there emerged a diel pattern containing a peak afternoon R value approximately 1.3 times that of R at night (Fig. 5 a,b). After an early morning dip in rates, R tracked almost linearly with P (although lagged in time by 0.5–1 h) as P rose and fell during the day (Fig. 6). Diel R based on the nighttime temperature relationship and/or the Q₁₀ function were also reasonable predictors of R_{exact} for part of the diel cycle. But these proxy R estimates deviated from the R_{exact} to varying degrees in both magnitude and timing, especially during the day (Figs. 7, 8) (see Table 3 footnote for definition of subscript notation). For one period (June C), the diel pattern of the Q₁₀-predicted R was the opposite of that indicated by the exact solution (Fig. 7). The differences between P_{exact} and P calculated from the various diel R proxies (constant R or temperature functions) in the mass balance approach were similarly variable during the day depending on the diel R assumption used. In some cases, the diel R proxy had little effect on P (September A–D2). Yet for other diel cycles (September C–D2) the assumed diel R changed the peak P relative to peak P_{exact} by up to 60% (Fig. 8).

The steady-state approximation was first used with O₂ and $\delta^{18}\text{O}_2$ at 10-min intervals using the optimized α_r to calculate instantaneous apparent P:R_{ss} ratios through the day (Fig. 9a). This form of the steady-state approach (Quay et al. 1995) failed to yield the correct instantaneous

P:R_{ss} ratio as calculated by the exact solution (P:R_{exact}). Disparities between P:R_{ss} and P:R_{exact} were greatest when the deviation from steady-state assumption was greatest (September; Fig. 9a). Lower P and smaller dO₂/dt in June led to closer agreement between P:R_{ss} and P:R_{exact}.

When the time-weighted daily mean O₂ and $\delta^{18}\text{O}_2$ values were used in the steady-state calculation, these P:R_{24,ss-dmv} ratios for the more heterotrophic conditions showed good agreement with P:R₂₄ ratios calculated using the other methods (Fig. 9b; Table 4). As with the other methods for calculating P:R₂₄, the P:R_{24,ss-dmv} approach identified Site A (June and September) as net heterotrophic, and Site C (September) as net autotrophic.

The time-forward model estimated metabolism parameters by defining model inputs (including the optimum α_r values) that yielded best fits of the modeled O₂ and $\delta^{18}\text{O}_2$ to the measured values. The model was run for September diel cycles, which contained the longest time series of data for calibration. Initial model calibration was done with constant R through the diel cycle. The output from these simulations could be made to match O₂ and $\delta^{18}\text{O}_2$ data during the day but deviated from measured $\delta^{18}\text{O}_2$ at night. R was redefined in the model as a function of either P or temperature. Good fits to the diel data were achieved by defining R as a function of P, but a unique best-fit set of parameters could not be established because of compensating gains and losses during the day. Simulations achieved the best fits to all O₂ and $\delta^{18}\text{O}_2$ data when R was defined as a function of temperature with a Q₁₀ of 1.42 (Fig. 10). The model yielded R₂₄ rates for September A and C of 7.23 and 8.29, mmol O₂ m⁻² h⁻¹, and P₂₄ rates for sites A and C of 5.25 and 8.88 mmol O₂ m⁻² h⁻¹ (Table 4), respectively. The resulting P:R₂₄ ratios for sites A and C (0.73 and 1.07) were similar to the P:R₂₄ values calculated

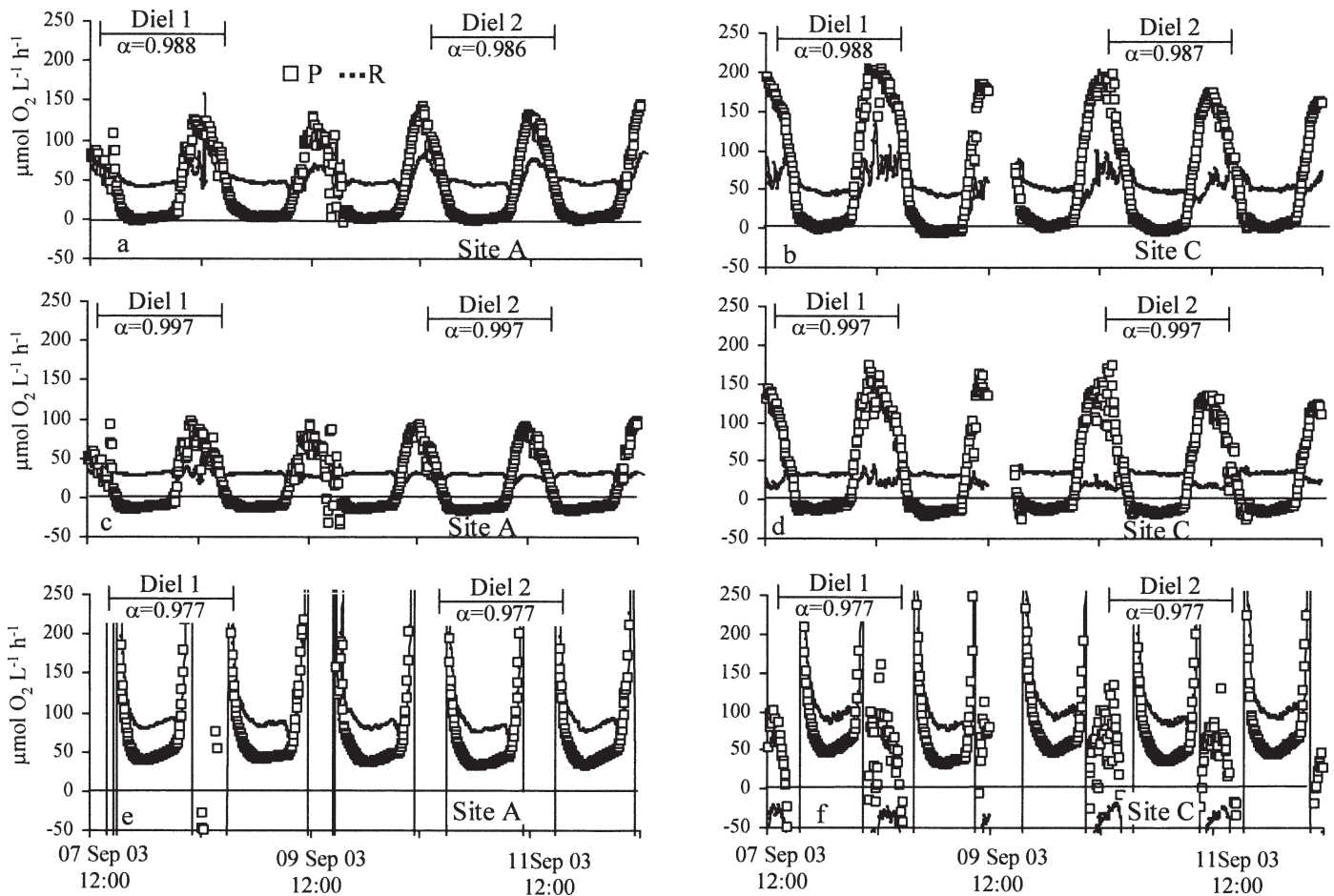


Fig. 5. Exact inverse solution estimates of P (large open squares) and R (small black squares) using different α_r values. (a, b) P and R rates estimated using best fit α_r values. See Fig. 2 for intervals represented by diel 1 and diel 2. (c, d) unreasonable values of nighttime P (< 0) for an assigned α_r of 0.997 (relatively transport-limited isotope fractionation). (e, f) unreasonable nighttime P (> 0) and erratic R for an assigned α_r of 0.977 (relatively enzyme-limited isotope fractionation).

using the mass balance and exact inverse solutions (Table 4). Although the model matched the amplitude and rate of change of the observed O_2 , the Q_{10} function used to define R caused the modeled O_2 to peak ~ 1 h after the observed O_2 . This mistiming is consistent with the results of the exact solution indicating that R peaked earlier than the Q_{10} function permitted. Model optimizations were done two different ways: (1) by fitting the O_2 concentration data first, then adjusting the value of α_r to fit the $\delta^{18}O_2$ data; and (2) by including α_r directly in the parameter optimization routine. The overall fits for normalized diel cycles of O_2 and $\delta^{18}O_2$ were about the same for both approaches at site A and about 7% better with the second approach at site C. Values of P were relatively unaffected, whereas the second approach yielded R values that were 3% and 7% higher at sites A and C, respectively, with correspondingly lower P:R₂₄ values. The mistiming of the modeled O_2 was not affected because it depended on the functional definition of R. As with the exact solution, poor model fits resulted when incorrect α_r values were assumed. For a given set of P and R values, changing the α_r caused the modeled $\delta^{18}O_2$ to deviate markedly from observed values (Fig. 10e,f).

Discussion

The multiple approaches used in Sugar Creek enabled us to evaluate some advantages and considerations for incorporating O_2 isotopes into aquatic metabolism studies. Specifically, we consider using $\delta^{18}O$ to estimate time variable R and examine the added uncertainty and overall value of adding isotopes to existing approaches.

Diel variation of R—The exact inverse solution required the most parameters (O_2 , $\delta^{18}O_2$, k_{O_2} , α_r) and provided the most information (variable P and R, and P:R ratios). This method independently estimated diel variation in R, which is not normally possible in most metabolism studies.

By estimating R directly during each measurement interval, we were able to compare the observed pattern to some of the functional representations of daytime R used commonly in open-channel diel studies. In June and September, each of the three proxies for diel R (constant R, $Q_{10} = 2$, or extrapolation from nighttime R vs. temperature), served as reasonable predictors for estimating instantaneous R at some point during the diel cycle, but no single proxy was able to reproduce the complete diel R

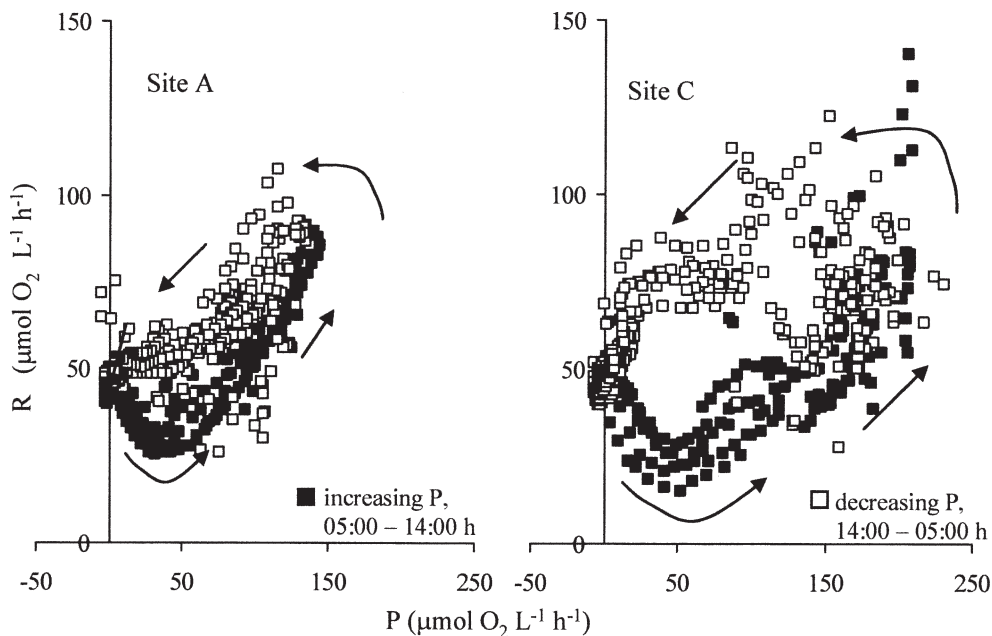


Fig. 6. Instantaneous R_{exact} as a function of P as calculated from the exact solution. Arrows indicate the direction of the diel cycle.

pattern calculated using the exact solution. From this limited number of samples we cannot generalize under what specific conditions the exact solution for diel R might improve the overall daily R , P , or $P:R_{24}$ estimates. The relative effect of assigning a specific proxy for diel R in lieu of using R_{exact} to calculate R_{24} , P_{24} , and $P:R_{24}$ varied from negligible to approximately 30% (Fig. 10; Table 4). The time-forward model also indicated that under certain circumstances where the diel R is reasonably well characterized by a temperature function, the addition of $\delta^{18}\text{O}_2$ may offer little additional advantage or improvement in the P_{24} , R_{24} , or $P:R_{24}$ estimates. For some sites in September, the appropriate temperature-based proxy for diel R yielded nearly identical P estimates as those calculated using the exact solution (Fig. 8). However, when the diel O_2 pattern cannot be fit well (e.g., in June), the isotopes can help to determine the appropriate diel R function (through the exact solution) and improve the overall model output. In June, when daylight conditions were the most variable, the relationship between temperature and R appears to have reversed over the course of the diel period. The use of a temperature function for diel R would not have reproduced the pattern. Therefore, the use of $\delta^{18}\text{O}_2$ to estimate diel variation in R has a number of potential uses: (1) to assess various options for functionalizing diel R within metabolism models and (2) for investigating the pathways and controls on respiration dynamics. Because of the sensitivity of R models to the value of α_r , more detailed studies of this type might reveal more about contributions of different respiration pathways (with different α_r values) and transport processes to the O_2 balance in aquatic systems.

Temperature and/or P likely had a role in controlling the diel cycle (daily rise and nighttime fall) in R . The inexact covariance between diel P and diel temperature makes it

difficult to isolate their effects on R . The R estimation from the exact solution followed a diel pattern that was best predicted by the various temperature-based proxies at night (Fig. 7). The relationship between R_{exact} and P was tightest during the day. Although a possible change in the temperature versus R functionality between night and day cannot be ruled out, it is likely that R shows at least some dependence on P (Pomeroy and Wiebe 2001). The patterns of R and P in Sugar Creek are consistent with environments where R is believed to be composed of low-level basal respiration that functions independent of P (at night), and a respiration component linked to P on short (daily) timescales (Baines and Pace 1991; del Giorgio and Williams 2005). The high daytime R could reflect increased heterotrophic respiration responding to labile dissolved organic carbon (DOC) exuded during P (Norrman et al. 1995) or accelerated photorespiration (e.g., Mehler-peroxidase or RUBISCO-oxidase reactions) accompanying high daytime irradiance and O_2 (Raven and Beardall 2005).

Sensitivity of the exact solution—There was a tradeoff between the added information provided by the O_2 isotopes and its data requirements and sensitivity. For the exact solution, periods of scatter in the calculated P and R record largely denote periods when the sampling interval was coarse relative to the change rate of O_2 and $\delta^{18}\text{O}_2$. In addition, the overall diel cycles in P and R were sensitive to the choice of α_r .

The values of α_r used in the exact inverse solution largely dictated the shape of the diel R curves, the baseline of the diel curves for P and R , and the overall stability of the solution (Fig. 5). Changes in α_r affected the integrated $P:R_{24}$ ratio as well as the individual magnitudes of P_{24} and R_{24} . The value of α_r had to be known within ± 0.002 to yield a complete time series set of solutions that were

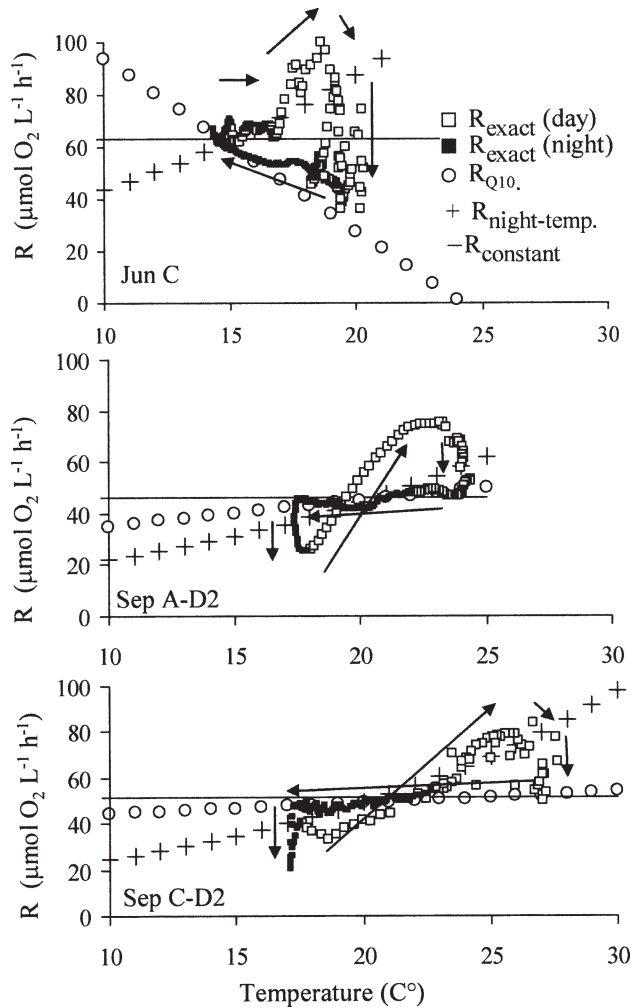


Fig. 7. Instantaneous R as a function of stream temperature. The R_{exact} values that were calculated using $\delta^{18}\text{O}_2$ (black and white squares), are compared to R values predicted by the three assumed functional relationships for R used in the mass balance only calculations. The nonexact R values are presented as (1) R is constant throughout the diel cycle (solid line); (2) R depends nonlinearly on temperature with $Q_{10} = 2$ (open circles); (3) R depends linearly on temperature and daytime R is extrapolated linear function of night R versus temperature (+ symbols). Arrows indicate the direction of the diel cycle.

consistent with value of zero for nighttime P . Most previously reported laboratory and water column values for α_r (typically around 0.980 ± 0.003) did not yield reasonable results for the time-forward simulation model or the exact inverse solution for any of the diel cycles. Both the diel models and the incubation experiments in this study indicate that the effective reach-scale α_r was larger (i.e., smaller fractionation effect) than typical enzyme-limited values for O_2 respiration. Although the incubation experiments provided evidence for relatively large values of α_r in the stream, they were of limited use in defining precisely the reach-scale value because of their variability (Table 2). The exact inverse solution and the time-forward model provided a means of optimizing for the appropriate system α_r that was not possible with the steady-state approaches. In

the absence of an optimization routine for α_r , benchtop fractionation experiments could be done but may not yield the appropriately precise system α_r . Differences between system α_r and laboratory α_r are not surprising given the possible contributions of different respiratory pathways that possess disparate α_r values (Raven and Beardall 2005) and possible transport limitations in the benthos including the hyporheic zone.

The Sugar Creek α_r values are significantly larger than those reported for respiration in enzyme-limited closed system experiments and other water column studies (0.982–0.977; Kiddon et al. 1993; Quay et al. 1995; Luz et al. 2002), but smaller than those reported for systems where O_2 respiration is largely limited by diffusion (e.g., 0.997; Brandes and Devol 1997). Because the Sugar Creek α_r values lie between the enzyme-limited and diffusion-limited endmembers, they may indicate partial transport limitation (Revesz et al. 1999) or represent the predominance of O_2 consuming pathways with larger α_r values. Chemical and/or microbial oxidation of reduced iron or sulfur in streambed pore waters could represent a mechanism of O_2 reduction with the requisite small isotopic fractionation effect ($\alpha_r = 0.982$ – 0.996 ; Taylor et al. 1984), but these reactions are not known to be a major component of total O_2 reduction in the stream. Alternate respiration pathways probably cannot solely explain the relatively small O_2 isotope fractionation either. The fractionation during photorespiration ($\alpha = 0.979$), the Mehler reaction ($\alpha = 0.985$), and alternative oxidase (AOX) pathways ($\alpha = 0.969$) are not small enough to explain the effective α_r s for Sugar Creek (Guy et al. 1993; Nagel et al. 2001) in the absence of at least partial transport limitation of the fractionation reaction. The effects of transport limitation on α_r may be linked to patterns of stream hydrology. Reach-scale O_2 removal represents the net effect of O_2 loss in different flowpaths that vary in transport limitation and reaction efficiency and thus vary in α_r . Hydrologic partitioning of this type has been used to explain the in situ fractionation patterns of NO_3^- isotopes at the watershed scale (Sebilio et al. 2003), and may have similar utility for explaining the effective system O_2 fractionation observed in Sugar Creek. Regardless of the controls on α_r , it is clear that assigning enzyme-limited α_r such as those measured or assumed in lakes or oceans was not appropriate. However, it should also be noted that our analysis assumes that α_r is constant through the diel cycle, which may not necessarily be true given the potentially varying contributions of alternative O_2 consuming pathways.

Application of the steady-state approximation for P: R—The steady-state solution has been, to date, the primary application of $\delta^{18}\text{O}_2$ measurements in metabolism studies (Quay et al. 1995; Wang and Veizer 2000; Russ et al. 2004). It has been applied generally to larger systems than Sugar Creek that more closely adhere to invariant O_2 concentrations. By comparing $P:R$ ratios calculated by the steady state and exact solutions for the different stream conditions in this study, we can examine in general terms the relative effect of diel O_2 variation ($d\text{O}_2/dt \neq 0$) on the typical application of the steady state solution. Secondly, by

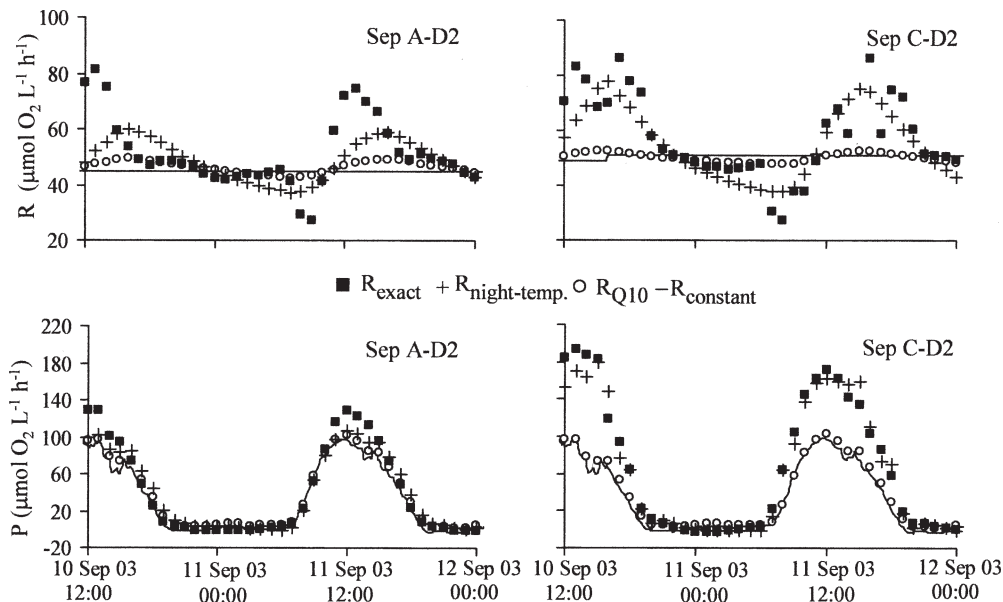


Fig. 8. Diel patterns of R and P estimated using the exact solution (solid squares) and the three formulations of diel R used in the mass balance only calculations (see Fig. 7 for description).

exploring an adaptation of the steady state solution using daily mean O_2 and $\delta^{18}O_2$ values (dmv) we can offer a possible approach for some non-steady state systems where knowing the $P:R$ ratio (without estimates of P or R) is deemed useful, and where diel O_2 , and $\delta^{18}O_2$ data can be collected, but gas transfer is difficult to quantify (e.g., large rivers or estuaries). The direct application of the steady-state approach (Quay et al. 1995) was useless in Sugar Creek when using discrete O_2 and $\delta^{18}O_2$ values selected from the diel cycle. There were at least two times during each diel cycle (early morning, and peak P in the afternoon) when dO_2/dt passed through zero and the $P:R_{ss}$ matched $P:R_{exact}$ (Fig. 9a). Knowing that $P:R = 0$ just before sunrise is not useful. Knowing the $P:R$ value at maximum

P is potentially interesting, but there was considerable scatter among $P:R_{ss}$ and $P:R_{exact}$ estimates at that time, and it was not practical to select the specific 10-min interval where O_2 and $\delta^{18}O_2$ values would yield $P:R_{ss}$ at parity with $P:R_{exact}$ (Fig. 9a). The failure of the steady-state approach using discrete data occurred in part because there were nonunique values of $\delta^{18}O_2$ for a given O_2 saturation state ($O_2/O_{2,s}$) that resulted from the non-steady-state conditions. The $\delta^{18}O_2$ values depended upon whether the O_2 was rising from a low nighttime concentration (high $\delta^{18}O_2$) or falling from a high daytime concentration (low $\delta^{18}O_2$). How much can a system deviate from steady state before the resulting $P:R_{ss}$ deviates significantly from the exact $P:R$? The deviation of instantaneous $P:R_{ss}$ from $P:R_{exact}$

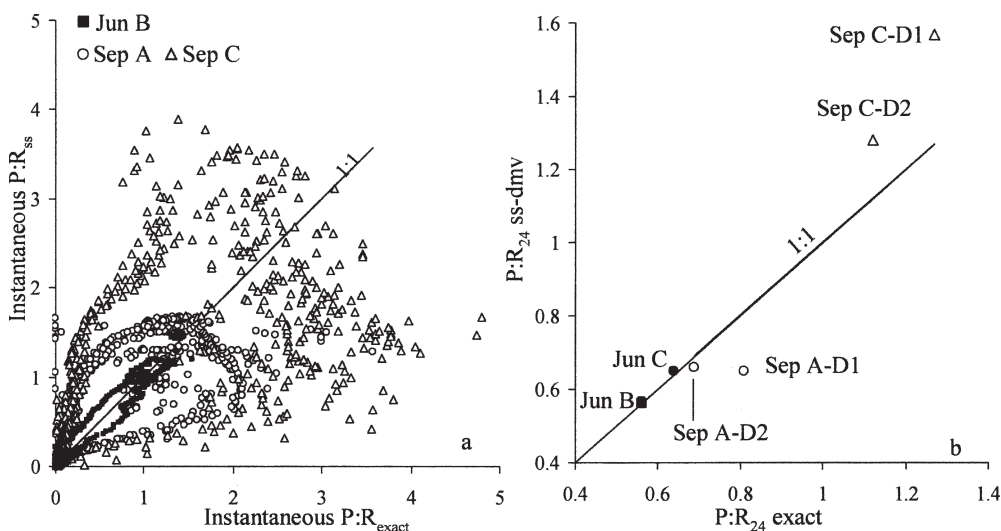


Fig. 9. Comparison of (a) instantaneous $P:R$ ratios and (b) daily $P:R_{24}$ ratios calculated using the exact solution and the steady-state (daily mean value) approaches.

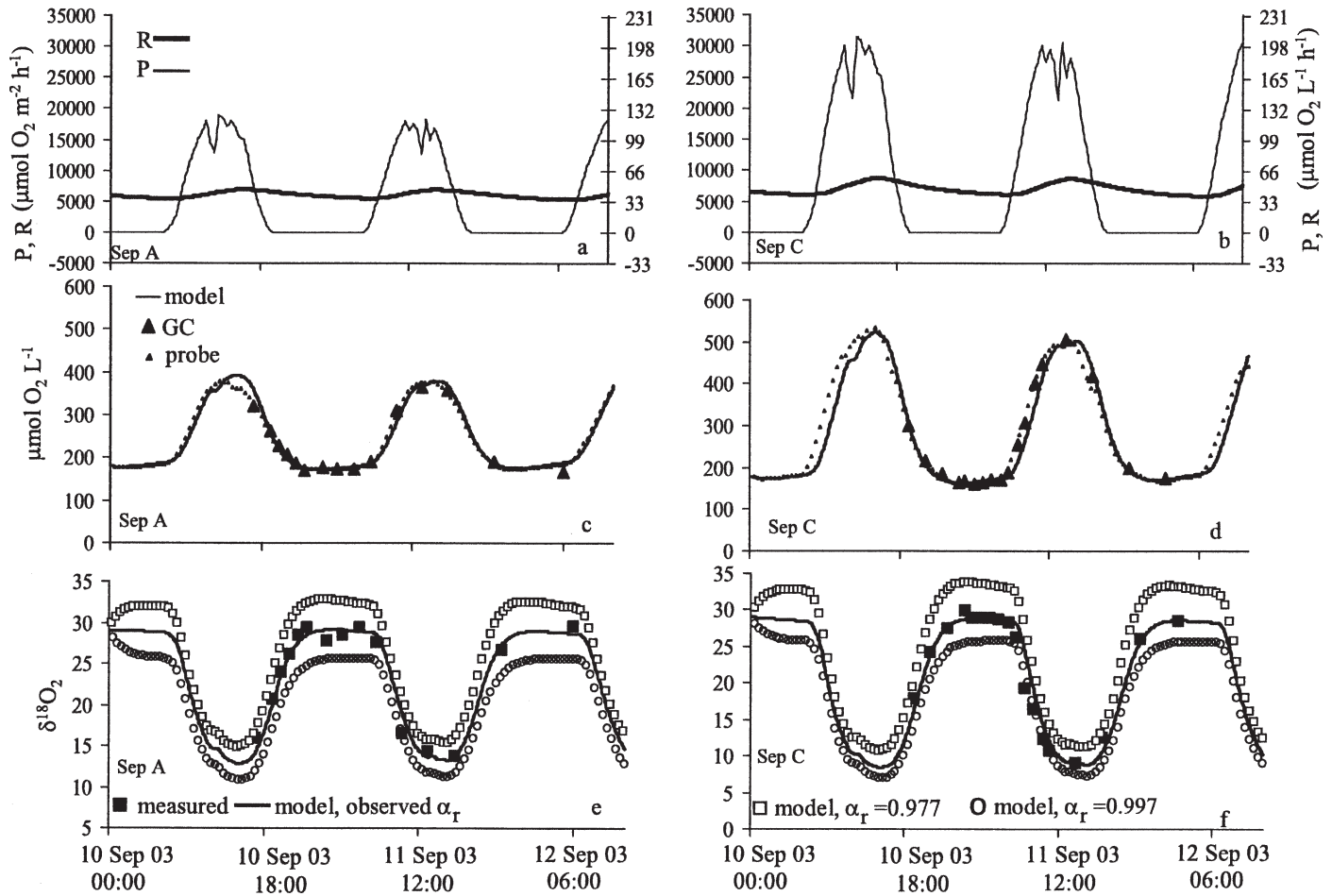


Fig. 10. Time-forward model results for September. (a, b) Modeled diel P and R values, (c, d) O_2 , and (e, f) $\delta^{18}O_2$ (in ‰ VSMOW). Solid lines indicate model output from the modeled best-fit of O_2 and $\delta^{18}O_2$ data using the optimum effective α_r of 0.989 and 0.987 for sites A and C, respectively. Solid symbols represent measured parameters. Large triangles are O_2 concentrations determined by GC, and small triangles are O_2 probe measurements. With the model optimized to fit only measured O_2 data, alternate α_r values were applied (e, f) to generate $\delta^{18}O_2$ output. Modeled $\delta^{18}O_2$ values illustrate the effect of substituting a relatively diffusion-dominated fractionation factor ($\alpha_r = 0.997$; open circles) or a relatively enzyme-limited fractionation factor ($\alpha_r = 0.977$; open squares) for the optimum α_r . When applying these nonoptimal α_r values, attempts to optimize model parameters using the $\delta^{18}O_2$ yielded model output that failed to fit measured O_2 and $\delta^{18}O_2$ data (simulations not shown).

corresponded to a ± 0.02 – 0.04 error in $P:R_{ss}$ for every $1 \mu\text{mol } O_2 \text{ L}^{-1} \text{ h}^{-1}$ deviation in dO_2/dt from zero. While this assessment sets boundaries on the use of the steady-state approach with discrete data from Sugar Creek, the relationship between dO_2/dt and $P:R_{ss}$ error will change with rates of P, gas transfer, and water depth in other environments. Even in systems with very low P and high gas transfer, the dO_2/dt may still deviate from zero because of variation of the O_{2sat} value in response diel temperature changes. In Sugar Creek this diel change in O_{2sat} accounted for a $5 \mu\text{mol } O_2 \text{ L}^{-1} \text{ h}^{-1}$ change in O_2/O_{2sat} ratio. Direct application of the steady-state solution using discrete values must therefore be restricted to thermally stable, low P (and or high gas transfer) environments that closely approximate steady-state conditions. An assessment of how well steady-state conditions must be adhered to under a variety of metabolic rates, gas transfer conditions, and assumed α_r values would help to constrain the use of the

steady-state solution in other systems, but it is beyond the scope of this current article.

When daily mean values of O_2 and $\delta^{18}O_2$ were used in the calculation, the resulting $P:R_{24,ss-dmv}$ closely approximated $P:R_{24-exact}$ for conditions that were net heterotrophic ($P:R_{24-exact} < 0.80$; Fig. 9b). This result is consistent with closer adherence to steady-state O_2 conditions under increasingly heterotrophic conditions where rates of changing O_2 concentrations and $\delta^{18}O_2$ are diminished. These limited results supported the possibility of using daily mean input parameters in the steady-state solution under conditions where P is low, the $P:R_{24}$ ratio is less than 0.7–0.8, and dO_2/dt is less than about $8 \mu\text{mol } O_2 \text{ L}^{-1} \text{ h}^{-1}$. The general applicability of the steady-state approaches is also limited by uncertainties in α_r . Unlike the exact inverse solution and the time-forward model, the steady-state approaches lack the capacity to optimize for the appropriate system α_r , and may thus be subject to larger errors in

P:R_{24ss} or P:R_{24,ss-dmv} estimates that arise from applying the wrong α_r . This effect is likely to be exacerbated in heterotrophic systems where R (and its α_r) control a larger portion of the overall O₂ budget.

In summary, incorporating O₂ isotopes into metabolism calculations offers the potential for improved characterization of diel variations in R, which may or may not translate into better metabolism estimates when compared to existing approaches. Independent estimation of R provided by the exact inverse solution is variably important to the overall metabolism estimates depending on how closely it is represented with alternate proxies for R. Direct measurement of diel R in and of itself represents an additional tool for investigating respiration dynamics. There is a trade-off between this additional information and potential error introduced by uncertainty in α_r . Whereas isotope-based calculations are highly sensitive to α_r , system α_r can be ascertained through optimization using the exact inverse solution and/or time-forward simulation model. For instances where k_{O_2} is not known, and P:R₂₄ only is desired, the steady-state solution (Quay et al. 1995) can be used provided that steady-state conditions are strictly adhered to ($dO_2/dt < 8 \mu\text{mol L}^{-1} \text{h}^{-1}$). The dmv approach to the steady-state solution (P:R_{24,ss-dmv}) can be applied to certain non-steady-state cases under conditions of net heterotrophy (e.g., P:R₂₄ < 0.70), where dO_2/dt integrated over a diel cycle approaches zero. The general applicability of the P:R_{24,ss-dmv} approach needs to be fully evaluated before it is generally adopted. All uses of $\delta^{18}O_2$ in metabolism calculations are sufficiently sensitive to α_r to require some quantification of a system-specific fractionation factor, especially in shallow systems where benthic processes are important. Evidence for diel variation in reach-scale α_r would complicate this approach further. The frequency and precision of the O₂ isotopic data could be improved in future studies to provide better characterization of hysteresis and tighter constraints on the models and possibly to evaluate temporal changes in α_r .

Given some uncertainties about the approaches used, some general conclusions from this study with respect to Sugar Creek, a small (2nd-order) stream in an agricultural watershed, include: (1) respiration decreased during the night and exhibited peaks during the day that were imperfectly correlated with temperature, possibly indicating additional controls related to P such as labile DOC production; (2) the reach-scale isotopic fractionation effect of O₂ reduction was less than most experimentally determined values, presumably because of benthic transport limitation or other factors; and (3) daily integrated values of P₂₄, R₂₄, and P:R₂₄ varied by up to 50% between sites spaced hundreds of meters apart, apparently because of reach-scale variations in abundance of benthic photosynthetic communities.

References

- BAINES, S. B., AND M. L. PACE. 1991. The production of dissolved organic matter by phytoplankton and its importance to bacteria: Patterns across marine and freshwater systems. *Limnol. Oceanogr.* **36**: 1078–1090.
- BENSON, B. B., AND D. KRAUSE JR. 1984. The concentration and isotopic fractionation of oxygen dissolved in freshwater and seawater in equilibrium with the atmosphere. *Limnol. Oceanogr.* **29**: 620–632.
- BÖHLKE, J. K., J. W. HARVEY, AND M. A. VOYTEK. 2004. Reach-scale isotope tracer experiment to quantify denitrification and related processes in a nitrate-rich stream, mid-continent United States. *Limnol. Oceanogr.* **49**: 821–838.
- BRANDES, J. A., AND A. H. DEVOL. 1997. Isotopic fractionation of oxygen and nitrogen in coastal marine sediments. *Geochim. et Cosmochim. Acta.* **61**: 1793–1801.
- COLE, J. J., M. L. PACE, S. R. CARPENTER, AND J. F. KITCHELL. 2000. Persistence of net heterotrophy in lakes during nutrient addition and food web manipulations. *Limnol. Oceanogr.* **45**: 1718–1730.
- DEL GIORGIO, P. A., J. J. COLE, AND A. CIMBLERIS. 1997. Respiration rates in bacteria exceed phytoplankton production in unproductive aquatic systems. *Nature.* **385**: 148–151.
- , AND R. H. PETERS. 1994. Patterns in planktonic P:R ratios in lakes: Influence of lake trophicity and dissolved organic carbon. *Limnol. Oceanogr.* **39**: 772–787.
- , AND P. J. LEB. WILLIAMS. 2005. The global significance of respiration in aquatic ecosystems: From single cells to the biosphere, p. 267–303. *In*: P. A. del Giorgio and P. J. leB. Williams [eds.], *Respiration in aquatic ecosystems*. Oxford Univ. Press.
- DUARTE, C. M., AND S. AGUSTI. 1998. The CO₂ balance of unproductive aquatic ecosystems. *Science.* **281**: 234–236.
- EPSTEIN, S., AND T. MAYDEA. 1953. Variation of ¹⁸O content of water from natural sources. *Geochim. Cosmochim. Acta.* **4**: 213–224.
- GUY, R. D., M. L. FOGEL, AND J. A. BERRY. 1993. Photosynthetic fractionation of the stable isotopes of oxygen and carbon. *Plant Physiol.* **101**: 37–47.
- HALL, R. O., JR., AND J. L. TANK. 2003. Ecosystem metabolism controls nitrogen uptake in Grand Teton National Park, Wyoming. *Limnol. Oceanogr.* **48**: 1120–1128.
- , AND ———. 2005. Correcting whole-stream estimates of metabolism for groundwater input. *Limnol. Oceanogr. Methods* **3**: 222–229.
- HANSON, P. C., D. L. BADE, S. R. CARPENTER, AND T. K. KRATZ. 2003. Metabolism: Relationships with dissolved organic carbon and phosphorous. *Limnol. Oceanogr.* **48**: 1112–1119.
- HORNBERGER, G. M., AND M. G. KELLEY. 1975. Atmospheric reaeration in a river using productivity analysis. *J. Environ. Engrg. Div ASCE* **101**: 729–739.
- JASSBY, A. D., AND T. PLATT. 1976. Mathematical formulation of the relationship between photosynthesis and light for phytoplankton. *Limnol. Oceanogr.* **21**: 540–547.
- KIDDON, J., M. L. BENDER, J. ORCHADO, D. A. CARON, J. C. GOLDMAN, AND M. DENNETT. 1993. Isotopic fractionation of oxygen by respiring marine organisms. *Global Biogeochem. Cycles* **7**: 679–694.
- KNOX, M., P. D. QUAY, AND D. WILBUR. 1992. Kinetic isotopic fractionation during air-water gas transfer of O₂, N₂, CH₄, and H₂. *J. Geophys. Res.* **97**: 20335–20343.
- LUZ, B., E. BARKAN, Y. SAGI, AND Y. Z. YACOBI. 2002. Evaluation of community respiration mechanism with oxygen isotopes: A case study in Lake Kinneret. *Limnol. Oceanogr.* **47**: 33–42.
- MARZOLF, E. R., P. J. MULHOLLAND, AND A. D. STEINMAN. 1994. Improvements to the diurnal upstream-downstream dissolved oxygen change technique for determining whole-stream metabolism in small streams. *Can. J. Fish. Aquat. Sci.* **51**: 1591–1599.

- MCCUTCHAN, J. H., JR., AND W. M. LEWIS. 2006. Groundwater flux and open-channel estimation of stream metabolism: Response to Hall and Tank. *Limnol. Oceanogr. Methods* **4**: 213–215.
- , J. F. SAUNDERS III, A. L. PRIBYL, AND W. M. LEWIS JR. 2003. Open-channel estimate of denitrification. *Limnol. Oceanogr. Methods* **1**: 74–81.
- , ———, W. M. LEWIS, JR., AND M. G. HAYDEN. 2002. Effects of groundwater flux on open-channel estimates of stream metabolism. *Limnol. Oceanogr.* **47**: 321–324.
- MULHOLLAND, P. J., J. N. HOUSER, AND K. O. MALONEY. 2005. Stream diurnal dissolved oxygen profiles as indicators of in-stream metabolism and disturbance effects: Fort Benning as a case study. *Ecol. Indicators* **5**: 243–252.
- , E. R. MARZOLF, J. R. WEBSTER, D. R. HART, AND S. P. HENDRICKS. 1997. Evidence that hyporheic zones increase heterotrophic metabolism and phosphorous uptake in forest streams. *Limnol. Oceanogr.* **42**: 443–451.
- , AND OTHERS. 2001. Inter-biome comparison of factors controlling stream metabolism. *Freshwater Biology* **46**: 1503–1517.
- NAGEL, O. W., S. WALDRON, AND H. G. JONES. 2001. An off-line implementation of the stable isotope technique for measurements of alternative respiratory pathway activities. *Plant Physiol.* **127**: 1279–1286.
- NORRMAN, B., U. L. ZWEIFEL, C. S. HOPKINSON, AND B. FRY. 1995. Production and utilization of dissolved organic carbon during an experimental diatom bloom. *Limnol. Oceanogr.* **40**: 898–907.
- ODUM, H. T. 1956. Primary production in flowing waters. *Limnol. Oceanogr.* **1**: 102–117.
- PACE, M. L., AND Y. T. PRAIRIE. 2005. Respiration in lakes, p. 103–121. *In*: P. A. del Giorgio and P. J. leB. Williams [eds.], *Respiration in aquatic ecosystems*. Oxford Univ. Press.
- PARKER, S. R., S. R. POULSON, C. H. GAMMONS, AND M. D. DEGRANDPRE. 2005. Biogeochemical controls on the cycling of stable isotopes of dissolved O₂ and dissolved inorganic carbon in the Big Hole River Montana. *Environ. Sci. Technol.* **39**: 7134–7140.
- POMEROY, L. R., AND W. J. WIEBE. 2001. Temperature and substrates as interactive limiting factors for marine heterotrophic bacteria. *Aquat. Microbial. Ecol.* **23**: 187–204.
- QUAY, P. D., D. O. WILBUR, J. E. RICHEY, A. H. DEVOL, R. BENNER, AND B. R. FORSBERG. 1995. The ¹⁸O:¹⁶O of dissolved oxygen in rivers and lakes in the Amazon Basin: Determining the ratio of respiration to photosynthesis rates in freshwaters. *Limnol. Oceanogr.* **40**: 718–729.
- RAVEN, J. A., AND J. BEARDALL. 2005. Respiration in aquatic photolithotrophs, p. 36–46. *In*: P. A. del Giorgio and P. J. leB. Williams [eds.], *Respiration in aquatic ecosystems*. Oxford Univ. Press.
- REVESZ, K., J. K. BÖHLKE, R. L. SMITH, AND T. YOSHINARI. 1999. Stable isotope composition of dissolved O₂ undergoing respiration in a ground-water contamination gradient. U.S. Geological Survey Water Resources Investigations Report 99-4018C, p. 323–328.
- RUSS, M. E., N. E. OSTROM, H. GANDHI, P. H. OSTROM, AND N. R. URBAN. 2004. Temporal and spatial variations in R:P ratios in Lake Superior, an oligotrophic freshwater environment. *J. Geophys. Res.* **109**: C10.
- SABATER, F. A., A. BUTTERINI, A. MARTÍ, I. MUNOZ, A. ROMANI, J. WRAY, AND S. SABATER. 2000. Effects of riparian vegetation removal on nutrient retention in a Mediterranean stream. *J.N. Am. Benthol. Soc.* **19**: 609–620.
- SEBILO, M., G. BILLEN, M. GRABLY, AND A. MARIOTTI. 2003. Isotopic composition of nitrate-nitrogen as a marker of riparian and benthic denitrification at the scale of the whole Seine River system. *Biogeochem.* **65**: 35–51.
- TAYLOR, B. E., M. C. WHEELER, AND D. K. NORDSTROM. 1984. Stable isotope geochemistry of acid mine drainage: Experimental oxidation of pyrite. *Geochim. et Cosmochim. Acta.* **48**: 2669–2678.
- WANG, X., AND J. VEIZER. 2000. Respiration-photosynthesis balance of terrestrial aquatic ecosystems, Ottawa area, Canada. *Geochimica et Cosmochim. Acta* **64**: 3775–3786.
- WEISS, R. F. 1970. The solubility of nitrogen, oxygen, and argon in water and seawater. *Deep-Sea Res.* **17**: 721–735.
- YOUNG, R. G., AND A. D. HURYN. 1998. Comment: Improvements to the diurnal upstream-downstream dissolved oxygen change technique for determining whole-stream metabolism in small streams. *Can. J. Fish. Aquat. Sci.* **55**: 1784–1785.
- , AND ———. 1999. Effects of land use on stream metabolism and organic matter turnover. *Ecolog. Appl.* **9**: 1359–1376.

Received: 3 January 2006
 Accepted: 17 February 2007
 Amended: 15 January 2007